This article has been accepted for publication in a future issue of this journal, but has not been fully edited. Content may change prior to final publication. Citation information: DOI 10.1109/TCE.2019.2932465, IEEE Transactions on Consumer Electronics

Design and Implementation of Smart Multi-Touch Interface Using Special Purpose CORDIC Processor

Ching-Iang Li, Gwo-Dong Chen, Tze-Yun Sung, and Huai-Fang Tsai

***Abstract*—This paper presents a smart and embedded multi-touch system for consumer electronics. The infrared (IR) camera is utilized to capture the coordinate of the IR blob from IR stylus or human finger in an emitted IR field. This system allows the consumer to easily convert large surface, projector screen, or conference table into multi-touch interface. The keystone distortion of IR camera is compensated by using homography. To improve the user experience, the calibration of homography is automatically triggered by accelerometer sensor. The special purpose (SP) processor with the parallel COordinate Rotation Digital Computer (CORDIC) architecture computes the observation-to-track association, and the computation result updates the motion status of each tracked trajectory. These motion data support the multi-touch tracking system to evaluate the sliding window of each tracked trajectory for reducing the tracking error. Additionally, the motion data are reused by the adaptive trajectory estimation (TE) system to smooth the touch trajectory and mitigate the measurement noise. This research presents multiple autonomous functions to provide a user-friendly multi-touch interface for consumer electronics. These include the automatic calibration system, the multi-touch tracking architecture with motion estimation system, and the adaptive TE system.**

***Index Terms*—CORDIC, Homography, Multi-touch interface, Trajectory estimation**

I. INTRODUCTION

The multi-touch device is a popular human-computer interface for consumer electronics such as smart phones, tablets, electronic whiteboards, and interactive projectors. Various multi-touch sensing methods are proposed. For example, the capacitive touch panel (CTP) is developed for the large size touch screen [1]–[3]. However, the capacitive sensors for large screen are difficult to transport and setup. On the other hand, this research selects the compact and portable multi-touch solution based on the IR camera as the hardware platform. Hence, the infrared (IR) camera multi-touch system allows a compact consumer device to simply overlay a multi-touch interface on a large surface such as conference table, whiteboard, and projector screen [4]–[6]. This is particularly useful for transforming the conventional display in office or classroom into the interactive multi-touch interface.

The development of multi-touch interfaces in consumer electronics includes the CTP and the IR light-emitting diode (LED) touch system [7]–[9]. These systems follow the architecture that converts the analog signal of the touch event to the coordinates, and the software tracking algorithms and the digital filters are applied. Likewise, the architecture of the IR camera system is divided into stages for capturing the IR signal and computing the touch coordinates. The basics of the IR camera touch system are demonstrated in the researches of multi-touch sensing through frustrated total internal reflection [10]–[12]. In detail, the IR camera is assembled by placing an IR-pass optical filter on a complementary metal-oxide-semiconductor (CMOS) camera sensor, and the narrow optical bandwidth produces distinct IR blob image with low ambient light noise. Thus, the IR stylus and the IR reflection of the human finger in an emitted IR field are captured as the IR blobs, and the touch event are accurately triggered. Liang *et al*. proposed an infrared optical technique for turning a display into a touch interface [13]. Similarly, Zhang *et al*. [14] and Hu *et al*. [15] proposed the camera-based finger detection method for the implementation of the touch interface. However, these researches show the computation of the touch coordinate is software-based, and their implementations require the host system to consume a large amount of the computational resources to compute the IR blob image. Song *et al*. utilized the chessboard pattern to calibrate the touch coordinate [16]. Hence, the homography is proposed to mitigate the keystone distortion of the camera-based touch screen [17], [18]. However, in these researches the calibration of the homography must completed manually.

The process for converting the IR blob into the touch coordinate is reducible to the classic connected components labeling problem. The captured frame is converted to an undirected graph, and the chained nodes are easily indentified via dynamic programming [19]. Therefore, the proposed system applies the connected components labeling algorithm [20] in the field-programmable gate array (FPGA) to improve the speed of the computation.

After the coordinates of the IR blobs are computed, homography [21] has been applied for the compensation of the keystone distortion, and the touch coordinates on the CMOS camera sensor are warped with respect to the physical position of

C.-I. Li and G.-D. Chen are with the Department of Computer Science and Information Engineering, National Central University, Taoyuan City, Taiwan (e-mail: 103582004@cc.ncu.edu.tw; chen@csie.ncu.edu.tw).

T.-Y. Sung and H.-F. Tsai are with the Aether Precision Technology Inc., Taoyuan City, Taiwan (e-mail: sung@aetherpt.com; st@aetherpt.com).

the graphical user interface (GUI). A key challenge of this operation is to define the feature points of the homography matrix. For finding these feature points, the pattern recognition algorithms based on the chessboard pattern and the circle pattern has been proposed [22], [23]. However, it is difficult to validate the correctness of the feature points in real-time.

When integrating these calibration methods into the consumer electronics, it is a challenge to request the consumer to manually perform the calibration procedure every time the physical orientation of the IR camera is altered. Thus, to improve the user-friendliness, the proposed system integrates an accelerometer sensor based on the microelectromechanical systems (MEMS) on the IR camera module. This low-cost accelerometer constantly monitors the physical orientation of the IR camera, and any variation to its gesture automatically triggers the calibration procedure in the resident program.

After the homography is computed, the touch coordinate sets in discrete sampling time must be associated by the coordinate tracking algorithm to link the touch trajectories. Traditionally, the approximate tracking result is derived by using the MDF algorithm or the Global Nearest Neighbor (GNN) approach, and the computation time is improved by the clustering method [8], [24]–[27]. However, the MDF algorithm is susceptible to faulty tracking results since defining a suitable gating threshold is difficult for low sampling rate device such as camera sensor [28]. When considering the large dimension of the proposed multi-touch interface and the limited frame rate of the IR camera, as the velocity of a touch trajectory increases, the displacement between the IR blobs in sequential frames may increase to a degree that makes the MDF algorithm insufficient for solving the coordinate tracking problem.

This research proposes the special purpose (SP) processor with the parallel COordinate Rotation Digital Computer (CORDIC) architecture that is embedded in the FPGA for the computation of the observation-to-track association. The CORDIC algorithm was originally developed by Volder [29] for 2-D rotation and polar coordinate transformation and substantially improved by Walther [30]. Indeed, the CORDIC algorithm is an efficient algorithm for computing the trigonometric functions in consumer electronics [31], [32]. The efficient hardware implementation of CORDIC is simple, and complex cells such as multipliers or dividers are not required [33], [34]. This work follows the multiple instruction, single data (MISD) type of parallel CORDIC architecture, and multiple operations are performed on the same input data in a single iteration [35]. In each CORDIC iteration, the accuracies of the distances and the angles between touch coordinates in sequential frames are computed and refined. This fixed-point architecture reduces the computation time by taking the advantage of the parallel architecture to conquer the large assignment matrix produced from large sets of touch coordinates.

The conventional multi-target tracking algorithm requires multiple sets of touch coordinates to be analyzed before producing the tracking decision [36], [37]. However, the touch interface demands rapid response time since the delay distance is visible on the GUI of the consumer electronics. In this research, the coordinate tracking algorithm is enhanced by utilizing the kinematic data to predict the sliding window of each trajectory. The Kalman filter is implemented to recursively observe the motion of each touch trajectory based on the result of the SP processor. Next, the gating decision maker evaluates sliding windows based on the estimation of velocity, displacement, and angular acceleration of each touch trajectory. The global optimal tracking decision is identified by applying the linear time selection algorithm to determine the best matching pairs in the observation-to-track matrix [38]. When tracking high velocity trajectory at low frame rate, the addition of the motion status in the gating decision reduces the tracking errors on the GUI of the consumer electronics.

After the coordinate tracking result is updated, the motion status of each trajectory is updated by the proposed SP processor, and the motion status is reused to perform the adaptive TE. The proposed TE system improves the smoothness of the touch trajectory on the GUI of the consumer electronics by mitigating the zigzag trajectory caused by the sensing error. This feature compensates inaccurate measurement noise of the IR blob since the IR signal quality is affected by the non-linear measurement error such as thermal noise, electrical noise, sensing error due to insufficient resolution, and disturbance of trembling hands. The recent researches of the TE for touch interface implemented the adaptive Kalman filter (AKF) [39], the fuzzy-logic-based adaptive strong tracking Kalman filter (FLASTKF) [40], and the particle filter (PF) [41]. However, the common characteristic of these TE methods is that the low filtering gain can create the distortion that easily sabotages the identity of the handwriting pattern. Hence, these methods are not suitable for filtering high velocity trajectory on large surface multi-touch interface. Thus, the proposed TE system is aimed to adaptively reduce the additional distortion while providing the TE function. The proposed TE system is designed to reuse the filtered motion status, and the fuzzy rules are defined to adaptively configure the filtering performance by observing the magnitude of the zigzag trajectory. Conveniently, the motion status of each finger allows the TE system to adaptively select the optimal Kalman gain (KG) to support filtering rapid handwriting trajectory on a large multi-touch interface. In this research the performance of the TE system is tested by following the evaluation of the writing stroke and the touch gesture [9]. It is shown that when the input trajectory is smooth, the adaptive TE system increases the KG to reduce the distortion, and as the measurement noise increases, the KG is decreased to compensate the zigzag trajectory.

The proposed system provides multiple autonomous functions to improve the user-friendliness of the multi-touch interface in consumer electronics. The main contribution of this research is summarized as follows:

1. The coordinate tracking system reduces the tracking error on the GUI by incorporating the motion data from the SP processor to estimate the sliding window and deliver the tracking decision.

2. The adaptive TE system smooth the touch trajectory by repurposing the motion data from the SP processor to supervise the smoothness of each trajectory and dynamically configure the filtering gain based on the magnitude of the zigzag trajectory.

This article has been accepted for publication in a future issue of this journal, but has not been fully edited. Content may change prior to final publication. Citation information: DOI 10.1109/TCE.2019.2932465, IEEE Transactions on Consumer Electronics

The combination of the above two features improves the usability of the multi-touch interface in consumer electronic by reducing the tracking error and measurement noise on the GUI. In addition, the proposed system is designed in an embedded hardware platform in order to preserve the valuable computational resource in the host system for the consumer. The application of the proposed system is not limited to the implementation of the IR camera system. In which, the proposed system is useful to accommodate the consumer devices such as the touch recognition system and the motion interactive system since the foundation of these systems is based on the accurately tracked touch trajectories.

The rest of the paper is organized as follows. In section 2, the hardware implementation of the proposed multi-touch system is shown. The section 3 describes the automatic calibration of the homography. The section 4 shows the FPGA SP processor with parallel CORDIC architecture. The section 5 presents the coordinate tracking system that is based on the sliding window estimation. The section 6 shows the adaptive TE system. The section 7 discusses the results of the implementation and the comparisons of the various researches. In section 8, the conclusion is given.

II. The Proposed Multi-Touch System

The implementation of the proposed IR Camera multi-touch system includes projector, IR camera module, MEMS accelerometer sensor, SP processor, and microcontroller unit (MCU), as shown in Fig. 1.

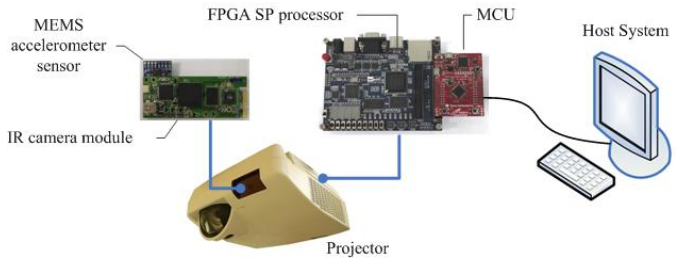

Fig. 1. The implementation of the proposed IR camera multi-touch system

The IR camera module is assembled with an IR-pass filter for filtering the ambient light, and the passing wavelength of the IR-pass filter is limited to a narrow 850 nm band. The 850 nm wavelength is used for implementing the IR laser emitter and the IR stylus. The MEMS accelerometer sensor is physically attached to the IR camera module for detecting its orientation, and any alteration to the gesture of the IR camera automatically triggers the calibration procedure to update the homography matrix. The embedded SP processor is designed with the parallel CORDIC architecture for the computation of the observation-to-track association. The MCU utilizes the computation result of the SP processor to perform coordinate tracking operation, adaptive TE, and zigzag trajectory detection. The USB interface on the MCU is connected to the host system, and it is recognized as a standard Human Interface Device (HID) and a USB Video Class (UVC) device, as shown in Fig. 2. Fig. 2 shows the software architecture in the host kernel and the resident calibration program. The standard multi-touch input driver recognizes the proposed system as a generic multi-touch device. The resident calibration program captures the camera image and transmits the configuration data to the proposed system via the UVC driver and the HID driver. This allows the realization of the automatic calibration function for updating the homography matrix.

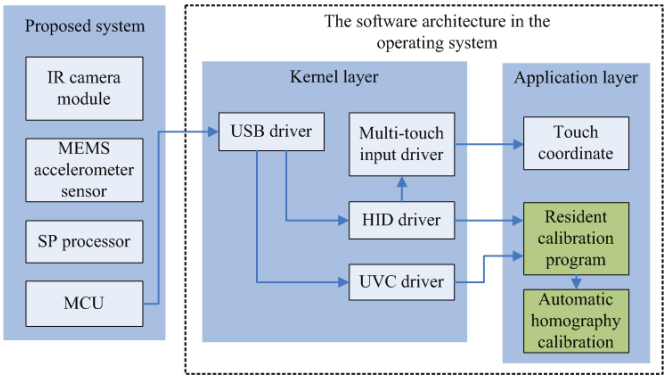

Fig. 2. The software architecture of the resident calibration program and the generic input system in the OS

III. The Automatic Calibration of Homography

The IR camera detects the coordinate of each IR blob with respect to the axle of the CMOS camera sensor. Thus, the homography matrix is applied to transform the image plane on the IR camera to the projected plane of the GUI. Fig. 3 shows the captured images from the IR camera, the size of the projected screen is 150 cm × 110 cm, and four feature points are used for applying the homography.

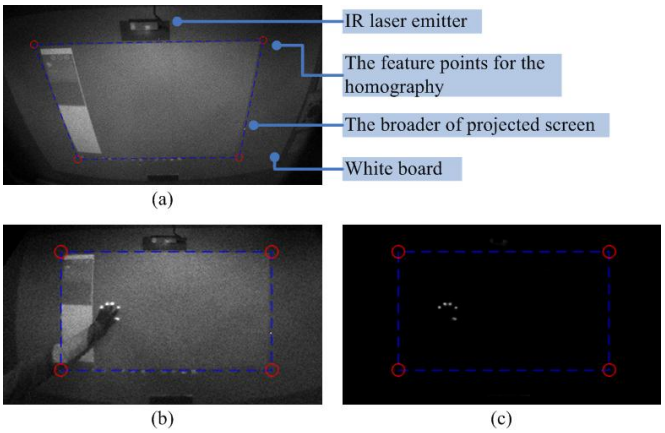

Fig. 3. The captured images from the IR camera module. The raw image without the IR-pass filter is shown in Fig. 3(a). In Fig. 3(b) and Fig. 3(c), the homography is applied, and the IR-pass filter is absent in Fig. 3(b) and present in Fig. 3(c)

Fig. 3(a) shows the raw image that is captured without the IR-pass filter. The rectified images are presented in Fig. 3(b) and Fig. 3(c), and a hand is placed on the same position of the screen. The red circles denote the feature points of the homography, and the dashed lines denote the broader of the screen. The IR laser emitter is utilized to emit a thin layer of laser curtain in front of the screen, and the IR laser reflection occurs when a touch contact is present. In addition, Fig. 3(c) shows the captured image with the IR-pass filter, and the reflection of the IR laser is clearly visible on each finger since the IR-pass filter eliminates the external light noise.

This article has been accepted for publication in a future issue of this journal, but has not been fully edited. Content may change prior to final publication. Citation information: DOI 10.1109/TCE.2019.2932465, IEEE Transactions on Consumer Electronics

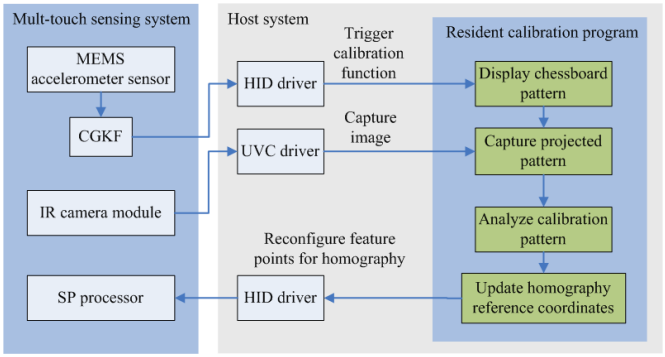

Fig. 4. The functional block diagram of the automatic calibration system for updating the homography matrix

Fig. 4 shows the proposed automatic calibration system for the compensation of the keystone distortion. When designing the consumer electronics, it is necessary to consider that consumers require a user-friendly interface for performing the calibration procedure. Thus, the proposed design improves the user experience of the consumer by integrating a MEMS accelerometer sensor to the IR camera module to detect any change to its physical orientation and the calibration procedure is automatically triggered.

In Fig. 4, the constant gain Kalman filter (CGKF) is implemented to estimate the orientation of the IR camera by filtering the measurement noise from the MEMS accelerometer sensor. When the MEMS accelerometer sensor detects the physical misalignment of the IR camera, the calibration system is triggered. Next, the host system is notified about the misalignment, and the HID report is passed to the resident calibration program to trigger the automatic calibration procedure in order to update the homography matrix. The resident calibration program displays the chessboard pattern on the GUI and captures the projected image from the UVC driver. The captured image is analyzed, and the feature points are generated based on the captured chessboard pattern, as shown in Fig. 5.

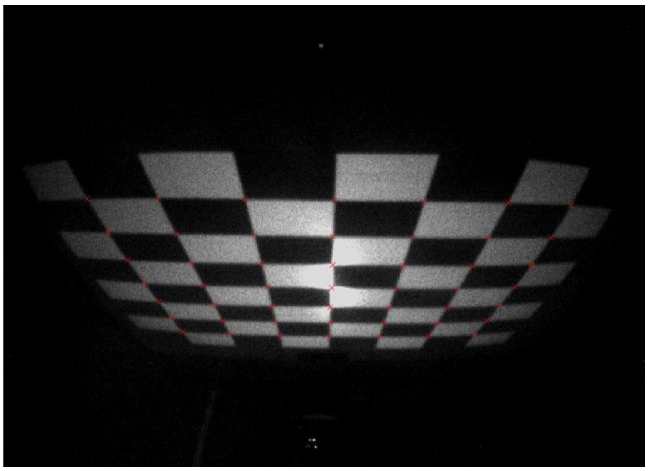

Fig. 5. The calibration of homography matrix

Fig. 5 shows the chessboard pattern displayed by the resident calibration program. The feature points of the homography are denoted as the red crosses, and their coordinates are passed to the proposed system for updating the homography matrix. Fig. 5 demonstrates the proposed system extracting 49 feature points from a single chessboard pattern. Overall, the proposed system is designed to automatically detect the misalignment of the IR camera and the homography matrix is always calibrated when the projector screen is within the field of view (FOV). Conveniently, this feature assists the consumer by eliminating the manual calibration procedure of the homography.

IV. The SP Processor With Parallel CORDIC Architecture

The proposed system exploits a parallel CORDIC architecture in the SP processor for the computation of the observation-to-track association. This design enhances the overall performance by reducing the execution time delay for tracking multiple touch contacts. The functional block diagram of the proposed multi-touch system and the SP processor is summarized in Fig. 6. In Fig. 6, each CORDIC processor

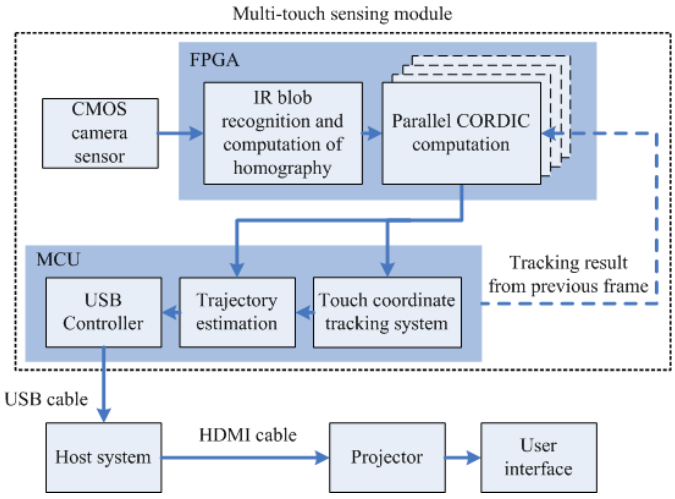

Fig. 6. The functional block diagram of the proposed multi-touch system and the SP processor

operates in the vectoring mode with the circular type of iteration. This architecture executes the MISD computation by solving the calculation of arctangent and distance between each member of the sampled sets in the sequential frames. This CORDIC implementation is scaling-free since the computation results are evaluated in the differential manner. The Cartesian coordinates from the two sampled sets in the sequential frames are defined as:

$$\left(x_\mu(j-1), y_\mu(j-1)\right),\ \left(x_m(j), y_m(j)\right) \quad (1)$$

where the (x, y) is the Cartesian coordinate of a touch contact and j is the index of time frame. The $\mu = 1, 2, 3, ...n(j-1)$ and $m = 1, 2, 3, ...n(j)$ are the indexes for the sets received at time frames $j-1$ and j. The distance and angle between all possible associations from the sets in time frames $j-1$ and j are evaluated in time frame j. The two observation-to-track matrixes with the size of $n(j-1)\times n(j)$ are generated. The distance and angle between two coordinates are solved in the following equations:

$$d_{m,\mu} = \sqrt{\left(x_\mu(j-1) - x_m(j)\right)^2 + \left(y_\mu(j-1) - y_m(j)\right)^2} \quad (2)$$

This article has been accepted for publication in a future issue of this journal, but has not been fully edited. Content may change prior to final publication. Citation information: DOI 10.1109/TCE.2019.2932465, IEEE Transactions on Consumer Electronics

$$\theta_{m,\mu} = \tan^{-1}\left(\frac{y_\mu(j-1)-y_m(j)}{x_\mu(j-1)-x_m(j)}\right) \quad (3)$$

where $d_{m,\mu}$ and $\theta_{m,\mu}$ are the distance and the angle between $\left(x_\mu(j-1), y_\mu(j-1)\right)$ and $\left(x_m(j), y_m(j)\right)$. Hence, the square root function and the arctangent function are resource-consuming computations that require long execution time in an embedded system. Thus, this work proposes an efficient solution based on the scaling-free CORDIC algorithm to compute the necessary square root function and arctangent function in MISD operations. The fundamental concept of the CORDIC algorithm decomposes the rotation of an angle β into a sequence of micro-rotations in an iterative manner, as shown below:

$$\beta = \sum_{i=0}^{\phi-1} \sigma(i)\cdot \tan^{-1} 2^{-i} \quad (4)$$

where ϕ is the iterations performed, $i = 0, 1, 2, 3....$ represents the index of each iteration, and $\tan^{-1} 2^{-i}$ is pre-calculated and stored in a look up table. The $\sigma(i) \in \{-1, 1\}$ denotes the direction of *i*-th micro-rotation. In this work, the CORDIC algorithm is configured in the vector rotation mode and the accumulation of the angle is in the circular coordinate system. The initialization of the CORDIC algorithm is as follows:

$$p(0) = \left|x_\mu(j-1)-x_m(j)\right| \quad (5)$$

$$q(0) = y_\mu(j-1)-y_m(j) \quad (6)$$

$$r(0) = 0 \quad (7)$$

where p, q, and r are CORDIC operators, and $p(0)$ is an absolute value because the convergence of the CORDIC algorithm for computing the arctangent function is only valid within the following range:

$$\sum_{t=0}^{\phi-1} \tan^{-1} 2^{-t} \approx 1.74 \quad (8)$$

Therefore, the range of r is defined as $[-\pi/2, \pi/2]$, and the recursive CORDIC operations are shown in the following equations:

$$For \quad i = 0 \quad to \quad \phi - 1, \quad Do$$

$$p(i+1) = p(i) + \sigma(i)\cdot 2^{-i}\cdot q(i) \quad (9)$$

$$q(i+1) = q(i) + \sigma(i)\cdot 2^{-i}\cdot p(i) \quad (10)$$

$$r(i+1) = r(i) - \sigma(i)\cdot \tan^{-1} 2^{-i} \quad (11)$$

$$End \quad i-loop$$

where $p(i)$, $q(i)$, and $r(i)$ are updated recursively, and $\sigma(i)$ is modified in each iteration according to the sign of $q(i)$, as shown below:

$$\sigma(i) = \begin{cases} -1 & q(i) \geq 0 \\ 1 & q(i) < 0 \end{cases} \quad (12)$$

The CORDIC computation efficiently uses simple shift-and-add operations. The accuracy of the CORDIC algorithm is depended on ϕ. According to the fixed-point error analysis of the CORDIC algorithm [35], the computation error is $\left(\sin^{-1}\left(\tan^{-1} 2^{-(\phi-1)} + \phi\cdot 2^{-\phi}\right)\right) + \phi\cdot 2^{-\phi}$. In this work, ϕ equals to the 16-bit word length, and $p(i)$, $q(i)$, and $r(i)$ converge to the following result:

$$p(\phi) = \left(\prod_{a=0}^{\phi-1}\sqrt{1+2^{-2a}}\right)\cdot\left(\sqrt{p(0)^2+q(0)^2}\right) \quad (13)$$

$$q(\phi) = 0 \quad (14)$$

$$r(\phi) = r(0) + \tan^{-1}\left(q(0)/p(0)\right) \quad (15)$$

where $\prod_{a=0}^{\phi-1}\sqrt{1+2^{-2a}}$ is a constant scaling factor since ϕ is constant. However, the proposed CORDIC algorithm is scaling-free since the tracking algorithm compares the distance between the coordinates in a differential manner. The results from (13) and (15) show the scaling-free CORDIC algorithm is implemented to compute the square root function in (2) and the arctangent function in (3). After the tracking result is updated, $p(\phi)$ becomes the velocity of a touch contact.

V. The Tracking System and Sliding Window Estimation

For each set in sequential frames, the multi-touch tracking system reports the track initiation, the track confirmation, and the track deletion. The three states are shown in the Venn diagram in Fig. 7. The concept of the tracking problem is to categorize sets of coordinate C in time frames j and $j-1$, and it is essential to produce the correct tracking decision since the tracking error can cause misoperation on the GUI of the consumer device. In Fig. 7, the solid circles are the coordinates in the set $C(j)$, and the hollow circles are the coordinates in the set $C(j-1)$. The goal of the tracking algorithm is to separate the two sets into the above three states and correctly

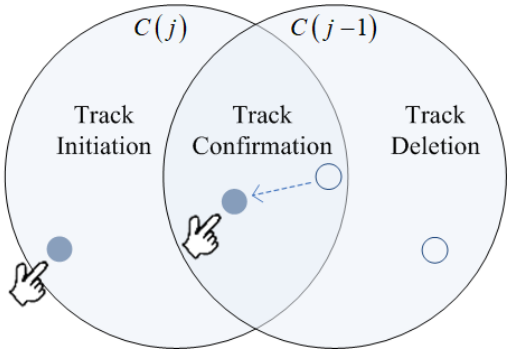

Fig. 7. The Venn diagram of the multi-touch tracking problem. Solid circles are the coordinates in the set $C(j)$, and hollow circles are the coordinates in the set $C(j-1)$. The goal of the tracking algorithm is to separate the two sets into the above three states and correctly link each confirmed track

This article has been accepted for publication in a future issue of this journal, but has not been fully edited. Content may change prior to final publication. Citation information: DOI 10.1109/TCE.2019.2932465, IEEE Transactions on Consumer Electronics

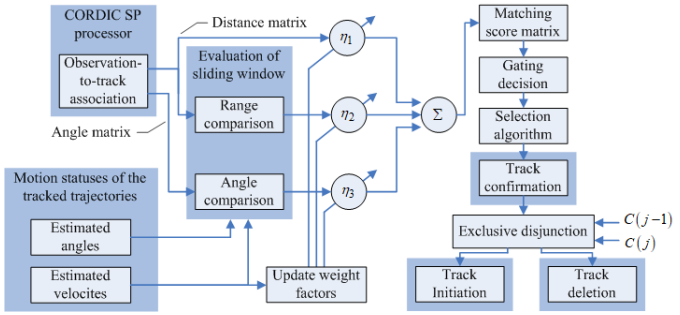

Fig. 8. The functional block diagram of the coordinate tracking system

link each confirmed track. The functional block diagram of the coordinate tracking system is shown in Fig. 8.

Fig. 8 shows the proposed coordinate tracking system evaluates the displacement, the estimated velocity, and the estimated directions of the trajectories to produce the tracking decision that is suitable for tracking high velocity trajectories. The proposed system utilizes the SP processor to perform the observation-to-track association, and the evaluation of the sliding window is accomplished by comparing the direction and the displacement of the tracklets to the angle and distance matrixes produced from the observation-to-track association. The η_1, η_2 ,and η_3 are the weight factors that are dynamically updated by evaluating the estimated velocities of the tracklets. At low velocity, the η_1 dominates the weights, and the tracking system performs similar to the MDF algorithm. As the velocity of the touch trajectory increases, the estimated direction converges, and the proposed system shift the weight distribution to η_2 and η_3 to evaluate the sliding window in the tracking decision.

After the tracking system generates the matching score matrix, the gating decision is applied to filter the invalid matching pairs, and the selection algorithm is utilized to produce the global optimal tracking decision by identifying the highest scores in the remaining sets. Thus, the track confirmation is reported, and the track initiation and deletion are completed by performing the exclusive disjunction operation. When the tracking system produces the tracking result, the velocity and the angular acceleration of each trajectory are recursively estimated by the Kalman filters, and the motion statuses of the tracked trajectories are updated. The tracking results of the proposed method and the MDF method are compared at 90 Hz, 60 Hz, and 30 Hz in Fig. 9. Fig. 9 shows, as the sampling rate decreases, the MDF algorithm produces faulty tracking result since its tracking decision is not provided with the enough intelligence of the trajectories.

Fig. 10 shows the intelligence of the tracklets that are evaluated by the fuzzy logic of the proposed tracking system. The solid dots denote the coordinates produced by sliding two fingers in parallel. Each circle represents the estimated range of the next displacement, and the dotted line shows the estimated direction of the trajectory. The estimated direction is inaccurate at low velocity since the raw data is unstable due to rapidly changing hand motion, yet the estimated direction stabilizes as the velocity increases. Furthermore, the estimated displacement ranges of the two trajectories are overlapped as the velocities of the fingers increases. The widely spaced displacement ranges

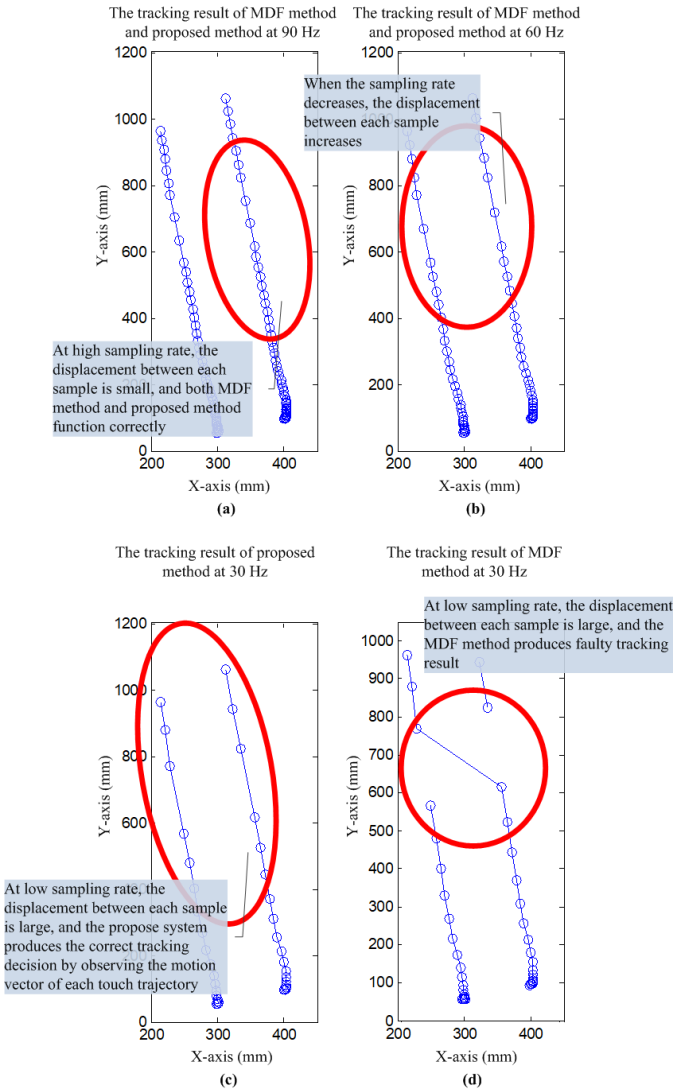

Fig. 9. The tracking results of (a) the proposed method and the MDF method at 90 Hz, (b) the proposed method and the MDF method at 60 Hz, (c) the proposed method at 30 Hz, and (d) the MDF method at 30 Hz

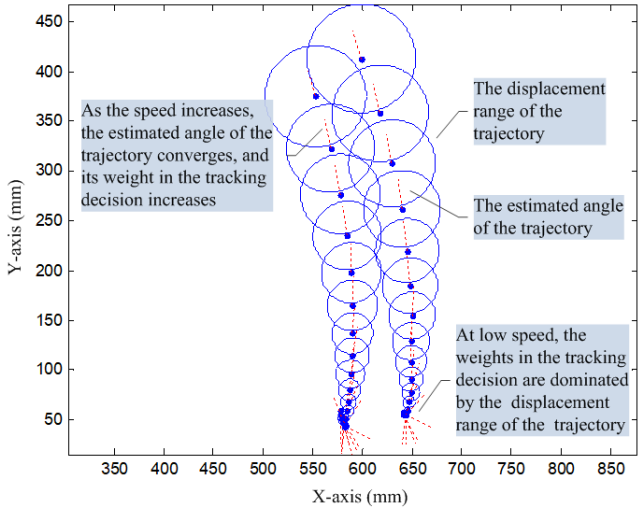

Fig. 10. The tracklets are evaluated by the fuzzy logic of the proposed tracking system. The solid dots denote the coordinates produced by sliding two fingers upward in parallel. The circles represent the estimated ranges of the next displacements, and the dotted lines show the estimated directions

This article has been accepted for publication in a future issue of this journal, but has not been fully edited. Content may change prior to final publication. Citation information: DOI 10.1109/TCE.2019.2932465, IEEE Transactions on Consumer Electronics

TABLE I
COMPARISON OF TRACKING SYSTEM FOR TOUCH INTERFACE

Method:	Tracking multiple trajectories at high velocity :	Performance evaluation:
Konstantinova *et al*. [27]	Poor	The GNN is a conventional multiple target tracking algorithm suitable for tracking widely spaced trajectories. The GNN produces tracking error when the velocities of the trajectories are high or the sampling rate is low.
Huang *et al*. [24]	Poor	The bipartite-matching method is implemented to improve the MDF algorithm for touch interface. However, the bipartite graph is inadequate for examining the closely spaced touch trajectories at high velocity.
Huang *et al*. [25]	Poor	The MDF method with the clustering algorithm is used for improving the computation speed for touch interface. However, the clustering decision is based on the minimum distance, and the faulty tracking result is produced when tracking multiple trajectories at high velocity.
This work	Better	This work produces tracking decision based on the fuzzy decisions and motion estimation. The angle, displacement, and velocity of the trajectory are evaluated by the fuzzy logic to reduce the tracking error. The proposed system supports tracking multiple trajectories at high velocity, and it is suitable for low sampling rate device such as IR camera.

cause the MDF algorithm to produce incorrect track confirmation. Table I compares the tracking method of the proposed system among various researches.

VI. THE ADAPTIVE TRAJECTORY ESTIMATION

The adaptive TE system is designed for mitigating the measurement noise and the undulation of the touch gesture. In fact, the TE system improves the smoothness of the touch trajectory which is clearly visible on the GUI of the consumer electronics.

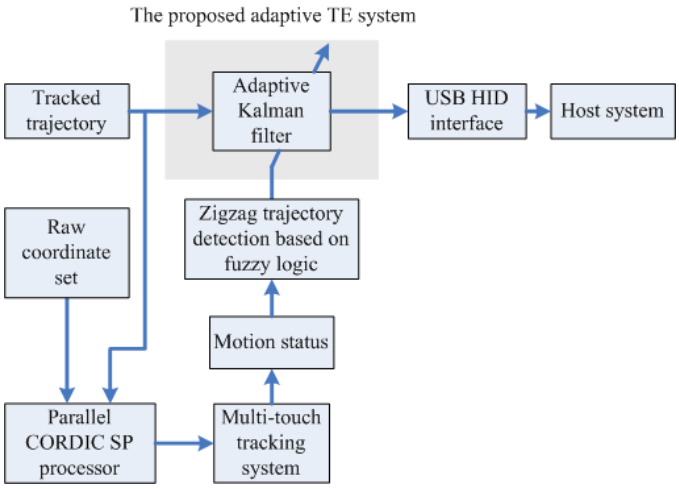

Fig. 11. The adaptive TE system.

Fig. 11 shows the functional block diagram of the adaptive TE system. The fuzzy logic is designed to measure the magnitude of the zigzag trajectory, and the result of the evaluation dynamically configures the filtering performance. The state estimation of the proposed TE system is shown as:

$$\dot{k}_f(j) = \dot{k}_f(j-1) + gain(j)\cdot\left(k_{in} - \dot{k}_f(j-1)\right) \quad (16)$$

where the current state estimation, $\dot{k}_f(j)$, is updated from the previous estimation, $\dot{k}_f(j-1)$, and the current input, k_{in}. The $gain(j)$ is the KG, and it is configured recursively by the fuzzy logic. The fuzzy rules are based on the sets of "If" and "then" statements, and at least one fuzzy rule is triggered for all input combinations. As the multi-input-single-output (MISO) decision maker, the fuzzy logic evaluates the estimated velocity and angular acceleration of a touch trajectory according to v and ω in the following membership functions:

$$v(k) = \{S, M, L\} \quad (17)$$

$$\omega(k) = \{Z, S, M, B, L\} \quad (18)$$

The output of the fuzzy membership function is U, and it is generated using the center-of-gravity method:

$$U(k) = \sum_{i=1}^{7} w_i r_i \Big/ \sum_{i=1}^{7} w_i \quad (19)$$

where r_i is the rule triggered, and w_i is the corresponding weight. The fuzzy membership functions are shown in Fig. 12, and Table II is the fuzzy arithmetic table. The fuzzy membership degree of U is defined as:

$$U(k) = \{SS, SM, SB, SL, LS, LM, LB, LL\} \quad (20)$$

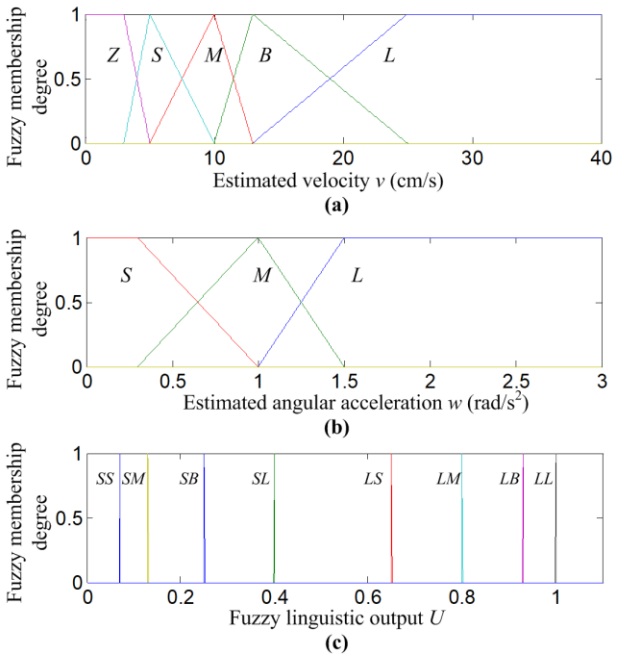

Fig. 12. The fuzzy membership degrees of (a) estimated velocity, (b) estimated angular acceleration, and (c) fuzzy linguistic output

This article has been accepted for publication in a future issue of this journal, but has not been fully edited. Content may change prior to final publication. Citation information: DOI 10.1109/TCE.2019.2932465, IEEE Transactions on Consumer Electronics

TABLE II
THE FUZZY ARITHMETIC TABLE

U: / v: / ω:	Z	S	M	B	L
S	LS	LM	LB	LL	LL
M	SB	SL	LS	LM	LB
L	SS	SM	SB	SL	LS

As shown in Fig. 13, when the magnitude of the zigzag trajectory increases, the KG is decreased to compensate the disturbance and improve the smoothness of the writing stroke. As the magnitude of the zigzag trajectory decreases, the proposed TE system increases the KG to minimize the distortion and the tracking delay distance, and the filtered result quickly converges to the raw trajectory. Table III shows the performance of the proposed TE system in comparison to the recent researches of the TE system for the touch interface. Fig. 14 shows the filtered result of the proposed TE system. The numeric characters are selected as the testing pattern for showing the rapidly changing motion of the touch gesture.

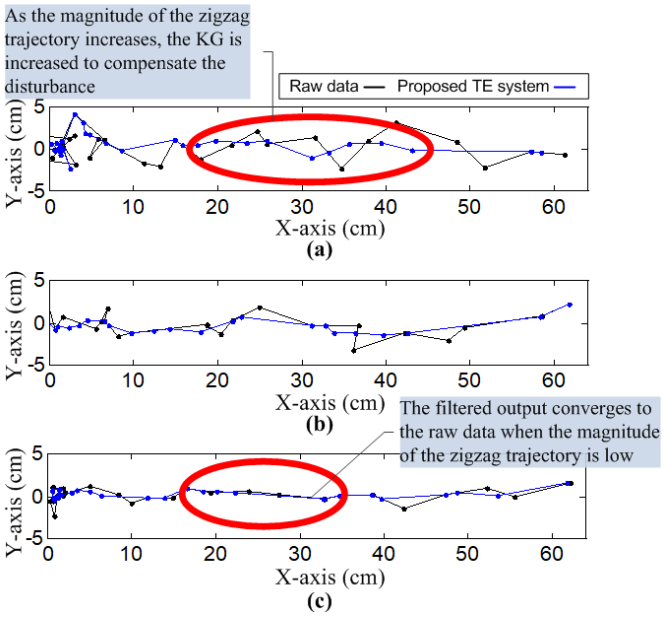

Fig. 13. The filtered results for mitigating the zigzag trajectories with the magnitude of (a) 5.3 cm, (a) 3.7 cm, and (c) 1.3 cm

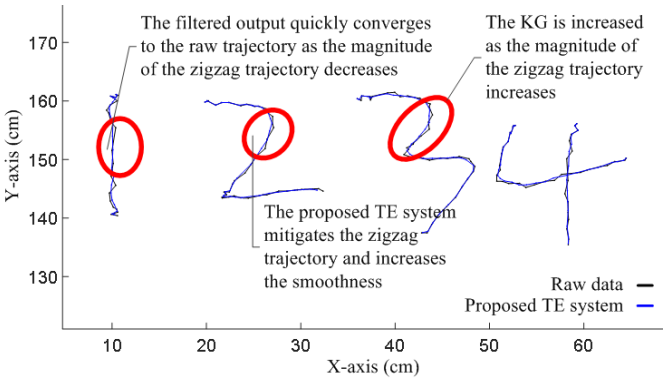

Fig. 14. The filtered nonlinear trajectories of the numeric characters.

VII. DISCUSSION

In the recent researches, the studies of the touch system for consumer electronics are focused on the CTP and IR LED technology [1]–[3], [8]. However, the panel sizes of these systems are in proportion to the size to the screen. In comparison, the hardware of the proposed IR camera system only consists of an IR camera and a SP processor module, and its physical form factor is very convenient to transport and install. Thus the proposed system enables a small and compact consumer device to support human-computer interaction on a large screen.

The proposed system introduces multiple autonomous functions to improve the user-friendless of the multi-touch interface in the consumer-electronics world. The MEMS accelerometer sensor is integrated in the proposed system for monitoring the orientation of the IR camera. This function assists the consumer by launching the calibration of the homography automatically. In contrast, the calibration procedures in previous works [11], [14], [15], [17] are manually performed at the expenses of consumers.

The SP processor is implemented as a multi-purpose computer to support both the coordinate tracking system and the TE system for accelerating the computation of observation-to-track association. In addition, the proposed system integrates the computation of IR blob detection, calibration, coordinate tracking, and TE in the embedded hardware in order to offload the computational resource from the host system. On the contrary, in the previous works, the

TABLE III
COMPARISON OF THE TE SYSTEM

Method:	Performance evaluation:
Lin *et al*. [40]	The FLASTKF produces distortion for filtering smooth trajectory with low measurement noise. The filtered result presents tracking delay and alteration of the original shape. This work only shows the performance of the filter at low speed.
Lin *et al*. [41]	The PF produces large tracking delay distance for filtering smooth trajectory. The implementation consumes large computational resource from the host system.
Lin *et al*. [39]	The AKF is not optimal for the implementation of touch interface since its filtered result does not converge to the raw data with low noise. The distortion is shown, and the curved testing pattern is deteriorated. This research only shows the performance for filtering the measurement noise at low speed.
This work	The proposed adaptive TE system mitigates the measurement noise by evaluating the magnitude of the zigzag trajectory. The testing pattern includes hand writings and zigzag trajectories with various magnitudes. The tracking delay distance for filtering smooth trajectory is low since the filtered trajectory quickly converges to the raw data as the magnitude of the zigzag trajectory decreases. The implementation utilizes the SP processor to offload the computational resource from the host system.

computation of the IR touch detection [13], finger detection [14], [15], and TE [41] requires the consumer device to share the precious process time and memory from the host system for computing the touch coordinate. The response time delay of the proposed system is 3.5 ms, whereas the finger detection system proposed by Hu *et al*. [15] has a response time delay of 20.9 ms, and the touch system from Dai et al. [17] has a response time delay of 30 ms.

The proposed coordinate tracking system utilizes the fuzzy logic and sliding window estimation to determine the tracking decision that is based on the estimation of the sliding windows. Thus, when tracking multiple high velocity trajectories, the proposed tracking system has the advantage over the MDF algorithm [24], [25], [27] that is implemented in the previous works of multi-touch system and consumer devices [8], [13], [15], [17]. The proposed TE system adaptively mitigates the inconstant measurement noise of the multi-touch system. In comparison to previous works [39]–[41], the filtered result produces smooth trajectory for filtering measurement noise, and as the magnitude of the measurement noise decreases, the proposed TE system quickly reduces its effect to decrease the distortion and prevent the alteration of the original touch pattern. The combination of these features gives the proposed system the feasibility to implement a large multi-touch interface using a simple IR camera module. Indeed, the tracking error and the measurement noise are visible on the GUI of the consumer device, and as the size of the screen increases, these errors are enlarged. This work uses FPGA as proof of concept for the implementation of the SP processor, in the future, it is planned to adopt the application-specific integrated circuit (ASIC) in the design.

VIII. Conclusion

This work discusses the IR camera multi-touch interface that is developed for the consumer electronics. Since the touch trajectory on the GUI is clearly visible to the consumer, this work proposes multiple autonomous functions to reduce tracking error and measurement noise of the multi-touch interface. Overall, the hardware of the multi-touch system is completed, and the real-time performance is very smooth. The application of this work is demonstrated using the IR camera, and in the future the proposed system has the potential for supporting other type of consumer electronics that rely on sensors to track trajectories. The examples include the human motion sensing system for virtual reality (VR) systems, game consoles, and autonomous vehicles.

References

[1] I. Yang and O. Kwon, "A touch controller using differential sensing method for on-cell capacitive touch screen panel systems," *IEEE Trans. Consum. Electron.*, vol. 57, no. 3, pp. 1027–1032, Aug. 2011.

[2] T. Hwang, W. Cui, I. Yang, and O. Kwon, "A highly area-efficient controller for capacitive touch screen panel systems," *IEEE Trans. Consum. Electron.*, vol. 56, no. 2, pp. 1115–1122, May 2010.

[3] Y. Park, J. Bae, E. Kim, and T. Park, "Maximizing responsiveness of touch sensing via charge multiplexing in touchscreen devices," *IEEE Trans. Consum. Electron.*, vol. 56, no. 3, pp. 1905–1910, Aug. 2010.

[4] J. Schoning, P. Brandl, F. Daiber, F. Echtler, O. Hilliges, J. Hook, M. Löchtefeld, N. Motamedi, L. Muller, P. Olivier, T. Roth, and U. V. Zadow, "Multi-touch surfaces: A technical guide," Technical University of Munich, München, Germany, Tech. Rep. TUM-I0833, 2008.

[5] P. Dietz and D. Leigh, "DiamondTouch: a multi-user touch technology," in *Symp. User Interface Software and Technology (UIST)*, Orlando, FL, USA, 2001, pp. 219–226.

[6] L. Dung, G. Lai, and Y. Wu, "Shadow touching for interactive projectors," in *2013 IEEE Int. Conf. Acoustics, Speech and Signal Processing*, Vancouver, BC, Canada, pp. 1798–802.

[7] J. K. Park, C. Lee, D. Kim, J. Chun, and J. T. Kim, "Application of weighing matrices to simultaneous driving technique for capacitive touch sensors," *IEEE Trans. Consum. Electron.*, vol. 61, no. 2, pp. 261–269, May 2015.

[8] B. Lee, I. Hong, Y. Uhm, and S. Park, "The multi-touch system with high applicability using tri-axial coordinate infrared LEDs," *IEEE Trans. Consum. Electron.*, vol. 55, no. 4, pp. 2416–2424, Nov. 2009.

[9] J. An, S. Hong, and O. Kwon, "A highly linear and accurate touch data extraction algorithm based on polar coordinates for large-sized capacitive touch screen panels," *IEEE Trans. Consum. Electron.*, vol. 62, no. 4, pp. 341–348, Nov. 2016.

[10] J. Y. Han, "Low-cost multi-touch sensing through frustrated total internal reflection," in *Symp. User Interface Software and Technology (UIST)*, Seattle, WA, USA, 2005, pp. 115–118.

[11] P. C. Ravoor, S. R. Rupanagudi, and B. S. Ranjani, "Detection of multiple points of contact on an imaging touch-screen," *2012 Int. Conf. Communication, Information & Computing Technology (ICCICT)*, Mumbai, India, pp. 1–6.

[12] K. Nakajima and T. Igarashi,"Full screen touch detection for the virtual touch screen," in *ACIVS 2017: Advanced Concepts for Intelligent Vision Systems*, Antwerp, Belgium, pp. 75–86.

[13] J. Liang, K. Lin, H. Chen, and W. Wang, "Turn any display into a touch screen using infrared optical technique," *IEEE Access*, vol. 6, pp. 13033–13040, Mar. 2018.

[14] L. Zhang, J. Saboune, and A. El Saddik, "Transforming a regular screen into a touch screen using a single webcam," *J. Display Technol.*, vol. 10, no. 8, pp. 647–659, Aug. 2014.

[15] J. Hu, G. Li, X. Xie, Z. Lv, and Z. Wang, "Bare-fingers touch detection by the button's distortion in a projector-camera system," *IEEE Trans. Circuits Syst. Video Technol.*, vol. 24, no. 4, pp. 566–575, Apr. 2014.

[16] C. Song , J. Cheng, and W. Feng, "A crowdsensing-based real-time system for finger interactions in intelligent transport system," *Wireless Communications and Mobile Computing*, vol. 2017, pp. 1–10, Oct. 2017.

[17] J. Dai and C. R. Chung, "Touchscreen everywhere: On transferring a normal planar surface to a touch-sensitive display," *IEEE Trans. Cybern.*, vol. 44, no. 8, pp. 1383–1396, Aug. 2014.

[18] K. Cheng and M. Takatsuka, "Initial evaluation of a bare-hand interaction technique for large displays using a webcam," in *Proc. 1st ACM SIGCHI symp. Engineering interactive computing systems (EICS '09)*, NY, USA, 2009, pp. 291–296.

[19] T. H. Cormen, C. E. Leiserson, R. L. Rivest, and C. Stein, *Introduction to Algorithms 3rd edition*. Cambridge, Massachusetts London, England: The MIT Press, 2009.

[20] C. T. Johnston and D. G. Bailey, "FPGA implementation of a Single Pass Connected Components Algorithm," in *4th IEEE Int. Symp. Electronic Design, Test and Applications (delta 2008)*, Hong Kong, China, pp. 228–231.

[21] O. Chum, T. Pajdla, and P. Sturm, "The geometric error for homographies," *Comput. Vis. Image Understand.*, vol. 97, no. 1, pp. 86–102, Jan. 2005.

[22] A. Geiger, F. Moosmann, O. Car, and B. Schuster, "Automatic camera and range sensor calibration using a single shot," in *Int. Conf. Robotics and Automation (ICRA)*, St. Paul, MN, USA, May 2012, pp. 3936-3943.

[23] J. Chu, A. GuoLu, and L. Wang, "Chessboard corner detection under image physical coordinate," *Optics and Laser Technology*, vol. 48, no. 1, pp. 599–605, Jun. 2013.

[24] S. L. Huang, S. Y. Hung, C. C. P. Chen, C. H. Tsao, and N. W. Chang, "An efficient multi-touch tracking algorithm with a large number of points," in *2014 IEEE 4th Int. Conf. Consumer Electronics Berlin (ICCE-Berlin)*, Berlin, Germany, pp. 429–430.

[25] S. L. Huang, S. Y. Hung, and C. P. Chen, "Clustering-based multi-touch algorithm framework for the tracking problem with a large number of points," in *2015 Design, Automation & Test in Europe Conf. & Exhibition (DATE)*, Grenoble, France, pp. 719–724.

[26] F. Wang, X. Ren, and Z. Liu, "A robust blob recognition and tracking method in vision-based multi-touch technique," in *2008 IEEE Int. Symp. Parallel and Distributed Processing with Applications*, Sydney, NSW, Australia, pp. 971–974.

[27] P. Konstantinova, A. Udvarev, and T. Semerdjiev, "A study of a target tracking algorithm using global nearest neighbor approach," in *Proc. 4th Int. Conf. Computer Systems Technologies: E-Learning*, Rousse, Bulgaria, 2003, pp. 290–295.
[28] K. Bernardin and R. Stiefelhagen, "Evaluating multiple object tracking performance: The clear MOT metrics," *EURASIP Journal on Image and Video Processing*, vol. 2008, no. 1, pp. 246–309, Feb. 2008.
[29] J. Volder, "The CORDIC trigonometric computing technique," *IRE Trans. Electron. Comput.*, vol. EC-8, no. 3, pp. 330–334, Sept. 1959.
[30] J. S. Walther, "A unified algorithm for elementary functions," in *Proc. Spring Joint Computer Conf. (AFIPS `71)*, Atlantic City, NJ, USA, 1971, pp. 379–385.
[31] J. Granado, A. Torralba, J. Chavez, and V. Baena-Lecuyer, "Design of an efficient CORDIC-based architecture for synchronization in OFDM," *IEEE Trans. Consum. Electron.*, vol. 52, no. 3, pp. 774–782, Aug. 2006.
[32] Z. Wu, J. Sha, Z. Wang, L. Li, and M. Gao, "An improved scaled DCT architecture," *IEEE Trans. Consum. Electron.*, vol. 55, no. 2, pp. 685–689, May 2009.
[33] P. A. Kumar, "FPGA implementation of the trigonometric functions using the CORDIC algorithm," in *2019 5th Int. Conf. Advanced Computing & Communication Systems (ICACCS)*, Coimbatore, India, pp. 894–900.
[34] T. Y. Sung, H. C. Hsin, and Y. P. Cheng, "Low-power and high-speed CORDIC-based split-radix FFT processor for OFDM systems," *Digital Signal Processing*, vol. 20, no. 2, pp. 511–527, Mar. 2010.
[35] T. Y. Sung and H. C. Hsin, "Design and simulation of reusable IP CORDIC core for special-purpose processors," *IET Comput. Digital Tech.*, vol. 1, no. 5, pp. 581–589, Sept. 2007.
[36] B. Benfold and I. Reid, "Stable multi-target tracking in real-time surveillance video," in *Proc. 2011 IEEE Conf. Computer Vision and Pattern Recognition*, Colorado Springs, CO, USA, pp. 3457–3464.
[37] S.S. Blackman, "Multiple hypothesis tracking for multiple target tracking," *IEEE Trans. Aerosp. Electron. Syst.*, vol. 19, no. 1, pp. 5–18, Jan. 2004.
[38] K. C. Kiwiel, "On Floyd and Rivest's SELECT algorithm," *Theoretical Computer Science*, vol. 347, pp. 214–238, Nov. 2005.
[39] C. L. Lin, T. C. Chu, C. E. Wu, Y. M. Chang, T. C. Lin, J. F. Chen, C. Y. Chuang, and W. C. Chiu, "Tracking touched trajectory on capacitive touch panels using an adjustable weighted prediction covariance matrix," *IEEE Tran. Ind. Electron.*, vol. 64, no. 6, pp. 4910–4916, Feb. 2017.
[40] C. L. Lin, Y. M. Chang, C. C. Hung, C. D. Tu, and C. Y. Chuang, "Position estimation and smooth tracking with a fuzzy-logic-based adaptive strong tracking kalman filter for capacitive touch panels," *IEEE Tran. Ind. Electron.*, vol. 62, no. 8, pp. 5097–5108, Jan. 2015.
[41] C. L. Lin, Y. M. Chang, H. S. Chen, C. Y. Chuang, and T. C. Chu, "Position tracking based on particle filter for self-capacitance single-touch screen panels," *J. Display Technol.*, vol. 11, no. 2, pp. 165–169, Oct. 2015.

Ching-Iang Li received the M.S. degree from the Department of Electrical Engineering, Yuan Ze University, Taoyuan City, Taiwan. Currently, he is a Ph.D. student in the Department of Computer Science and Information Engineering in the National Central University, Taoyuan City, Taiwan. His research fields include control system, sliding mode control, fuzzy system, embedded computer system, and VLSI design.

Gwo-Dong Chen received the B.S., M.S., and Ph.D. degrees in electrical engineering from the National Taiwan University, Taipei City, Taiwan in 1991. He is now the chief executive for the Aim For The Top University Project and also the chair professor at the Department of Computer Science and Information Engineering in the National Central University, Taoyuan City, Taiwan. His research has been devoted to human-computer interaction, interactive Learning software design, and cognitive systems and he has published more than 150 research papers.

Tze-Yun Sung received the Ph.D. degree in electrical engineering from National Taiwan University, Taipei City, Taiwan, in 1987. He was a Professor with the Department of Electronics Engineering, Chung Hua University, Hsinchu City, Taiwan. Currently, he is the president of Aether Precision Technology Inc., Taoyuan City, Taiwan. His research interests include VLSI design, VLSI signal processing, computer arithmetic, computer organization, image compression, image processing, computer vision, and medical devices and he has published more than 200 research papers.

Huai-Fang Tsai received the M.S. degree from the Institute of Electro-Optical Engineering, National Chiao Tung University, Hsinchu, Taiwan. Currently, he is the CTO of Aether Precision Technology Inc., Taoyuan City, Taiwan. His research fields include the photonic sciences and the optical system. His has been devoted to the R&D and the manufacturing process of the diffraction optical element.